

Supplementary information for

Multicomponent Equimolar Proton-Conducting Quadruple Hexagonal Perovskite-Related Oxide

Abid Ullah^{a,b,‡}, Huaasain Basharat^{a,b,‡}, Yong Youn^{c,‡}, Hyung-Bin Bae^d,
Jong-Eun Hong^a, Dong Woo Joh^a, Seung-Bok Lee^a, Rak-Hyung Song^a, Tae Woo Kim^a,
Tak-Hyoung Lim^{*a} and Hye-Sung Kim^{*a}

^a*High Temperature Energy Conversion Laboratory, Korea Institute of Energy Research,
Daejeon 34129, Korea*

^b*Department of Advanced Energy and System Engineering, University of Science and Technology,
Daejeon 34129, Korea*

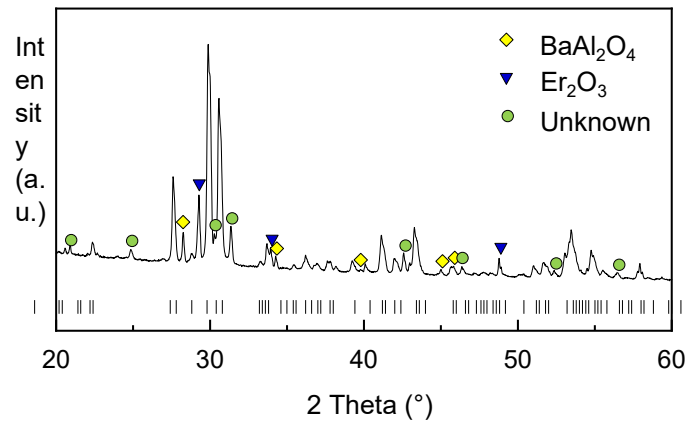
^c*Computational Science & Engineering Laboratory, Korea Institute of Energy Research,
Daejeon 34129, Korea*

^d*KAIST Analysis Center for Research Advancement, Korea Advanced Institute of Science and
Technology, Daejeon 34341, Korea*

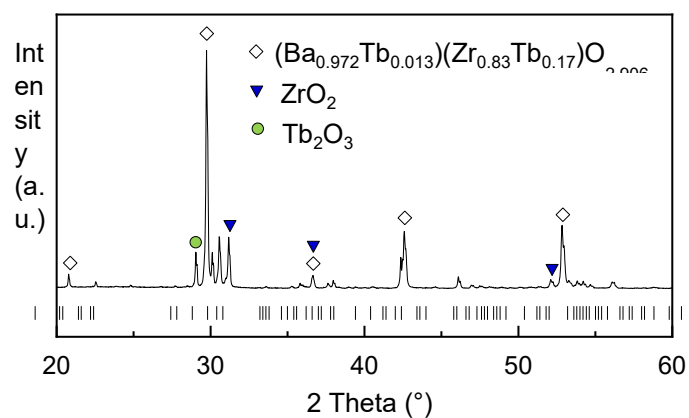
* Corresponding author:

E-mail address: hsk@kier.re.kr (H.-S. Kim) and ddak@kier.re.kr (T.-H. Lim)

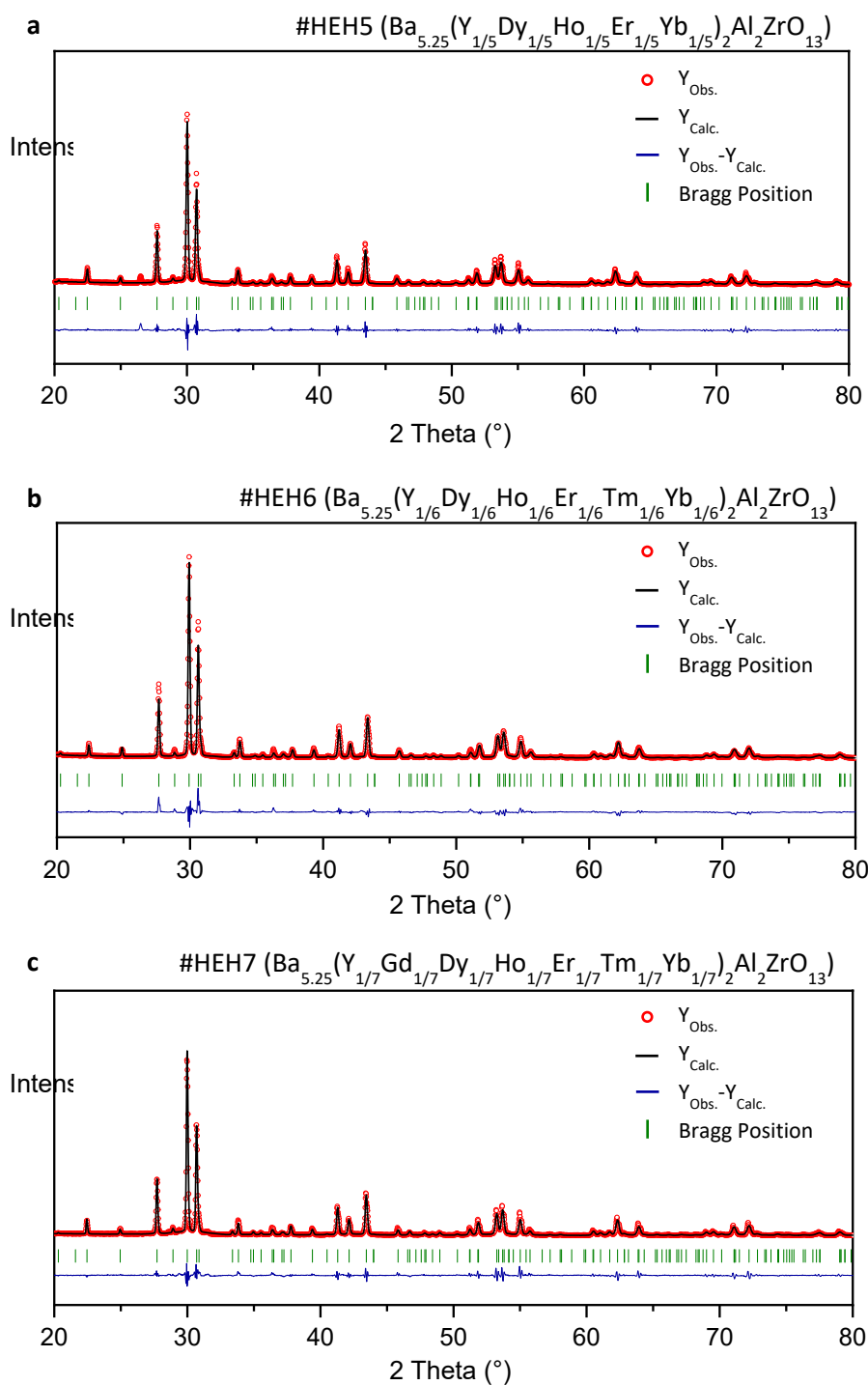
‡The co-first authors Abid Ullah, Hussain Basharat and Yong Youn contributed equally to this work



Supplementary Figure 1. X-ray diffraction pattern of the powder in contact with the Al_2O_3 crucible used in the second heat treatment process (1600°C for 10 h) for the BRAZ synthesis. Non-negligible amounts of BaAl_2O_4 (yellow diamond), Er_2O_3 (blue inverted triangle), and unknown (green circle) peaks were identified along with the BRAZ main peaks. Reference XRD peaks based on the BEAZ structure are shown at the bottom of the graph for a better comparison.

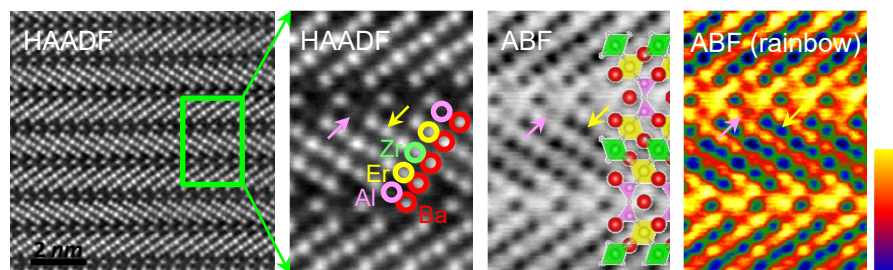


Supplementary Figure 2. X-ray diffraction results of the $\text{BaTb}_2\text{Al}_2\text{ZrO}_{13}$ powder. When a divalent Tb element is added to the Re-site, the system becomes a combination of various secondary phases with $(\text{Ba}_{0.972}\text{Tb}_{0.013})(\text{Zr}_{0.83}\text{Tb}_{0.17})\text{O}_{2.906}$ (yellow diamond), ZrO_2 (blue inverted triangle), Tb_2O_3 (green circle), and several unknown peaks as the main structure rather than the P63/mmc hexagonal perovskite structure. Reference XRD peaks based on the BEAZ structure are shown at the bottom of the graph for a better comparison.

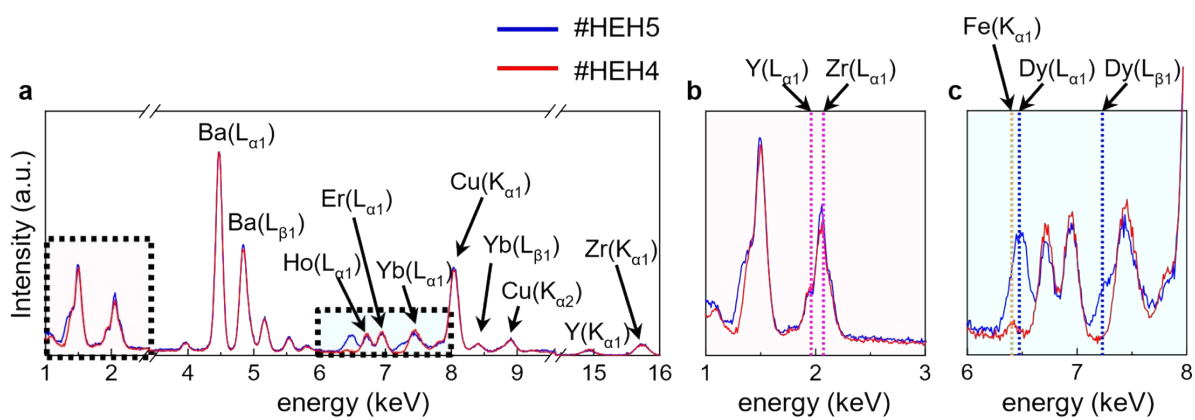


Supplementary Figure 3. Rietveld refinement of (a) #HEH5, (b) #HEH6 and (c) #HEH7 powder. The calculated and observed patterns are shown in the top by solid black line ($Y_{\text{Calc.}}$) and red dots ($Y_{\text{Obs.}}$), respectively. Thick vertical below the patterns represent the

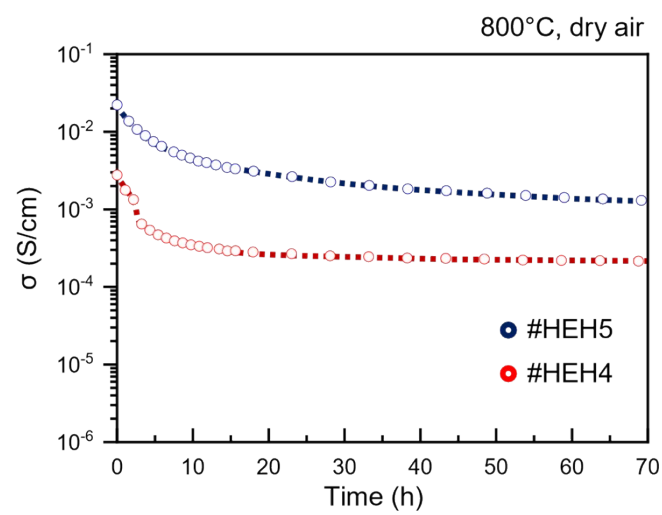
position of all possible Bragg reflections. The trace in the bottom is a plot of the difference between the observed and calculated intensities ($Y_{\text{Obs.}} - Y_{\text{Calc.}}$).



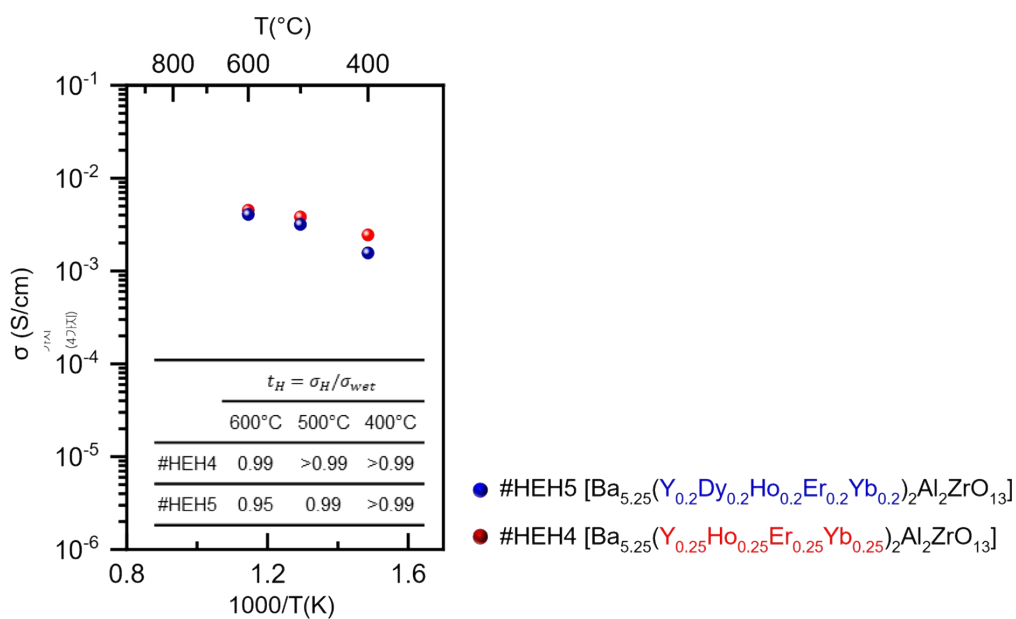
Supplementary Figure 4. HAADF-, ABF- and rainbow scale ABF-STEM images of $\text{Ba}_{5.25}\text{Er}_2\text{Al}_2\text{ZrO}_{13}$ in the [100] hexagonal direction. The white arrow in HAADF-STEM magnified in the green dotted box area indicates the position of Ba in the h:BaO layer, and the pink arrow indicates the Al position, and the yellow arrow indicates the position of Er in the c:BaO layer. The position of each element was overlaid on the magnified HAADF-STEM image, and the crystal structure was overlaid on the right side of the ABF-STEM image.



Supplementary Figure 5. (a) Energy-dispersive X-ray spectroscopy spectrum of #HEH5 (blue solid line) and #HEH4 (red solid line). The two spectrums were normalized based on their intensity of the BaL_{α1} peaks and were plotted with arbitrary units. (b) Magnified EDS spectrum from 1 to 3 keV presents the indistinguishable X-ray energy of the Y-L_{α1} (1.924 keV) and Zr-L_{α1} (2.044 keV) peaks and those two peaks are indicated by a pink dotted line. (c) The presence of Dy in #HEH5 was clearly confirmed through a magnified EDS spectrum from 6 to 8 keV. The intensity of Cu-K_{α1} in (a) and Fe-K_{α1} in (c) are the artifacts caused by the sample grid and TEM devices.



Supplementary Figure 6. Electrical conductivity over time in dry air at 800°C.



Supplementary Figure 7. Arrhenius plot for the pure protonic conductivity (t_H) of #HEH5 and #HEH4.

Inside the graph, the protonic transference number values at 600°C, 500°C, and 400°C for the two systems are presented. Both systems show pure ionic conductor properties at below 500°C.

Supplementary Table 1. Characteristic X-ray energies of the various elements.

Z	Element	X-ray energy (keV)					
		K α_1	K β_1	L α_1	L β_1	M α_1	M β_1
13	Al	1.486	1.557				
26	Fe	6.405	7.059	0.705	0.718		
29	Cu	8.046	8.904	0.928	0.947		
39	Y	14.958	16.739	1.924	1.998		
40	Zr	15.775	17.668	2.044	2.126		
56	Ba	32.194	36.378	4.466	4.828		
60	Nd	37.361	42.272	5.228	5.719		
62	Sm	40.118	45.414	5.633	6.201		
63	Eu	41.542	47.038	5.849	6.458		
64	Gd	42.996	48.695	6.053	6.708		
66	Dy	45.999	52.113	6.498	7.248	1.293	1.325
67	Ho	47.547	53.877	6.720	7.526	1.348	1.383
68	Er	49.128	55.674	6.949	7.811	1.404	1.448
69	Tm	50.742	57.505	7.180	8.102	1.462	1.503
70	Yb	52.388	59.382	7.416	8.402	1.526	1.573